

An improved thermal network model of the IGBT module for wind power converters considering the effects of base plate solder fatigue

H Li^{1,4}, Y G Hu^{1,4}, S Q Liu², Y Li¹, X L Liao¹ and Z X Liu³

¹The State Key Laboratory of Power Transmission Equipment & System Security and New Technology (Chongqing University), Chongqing, China

²The State Grid Jiangxi Electric Power Corporation Ganzhou Power Supply Company, Ganzhou, China

³Chongqing KK-QIANWEI Wind Power Equipment Co., Ltd, Chongqing, China

E-mail: cqulh@163.com, huyaogang345@163.com

Abstract. This study presents an improved thermal network model of the IGBT module that considers the effects of base plate solder fatigue on the junction temperature of the said module used in wind power converters. First, the coupling thermal structure 3D finite element model of the IGBT module is established based on the structure and material parameters of the module used in the wind power converters of a doubly fed induction generator. The junction temperature of the module is also investigated at different thermal desquamation degrees of the base plate solder. Second, the thermal resistance parameters are determined at different desquamation degrees, and the improved thermal network model that considers the effects of base plate solder fatigue is established. Finally, the two results of the calculation of the junction temperature are compared in different fatigue stages through the improved thermal network model and the 3D finite element model, which testify to the effectiveness of the improved thermal network model.

1. Introduction

As an energy transfer interface, the wind power converter is the core component of large power wind turbines. Given the successful development of wind farms and particularly offshore wind turbines [1-2], some critical components of gearbox, generator, and power converter are subjected to serious operational environments. Especially power converters are also prone to drastic thermal stress shocks, such as the continuous random torque in wind turbines. The safe operation and reliability of wind power converters have received increase attention in recent years [3-5]. The reliability of IGBT modules, which highly depend on accurate information on the junction temperature, is vital for power converters and the whole wind turbine system [5]. A thermal network model, such as a foster network, is generally used to calculate the junction temperature of an IGBT module [4, 6]. However, the thermal stress between different materials results in the desquamation of the base plate solder, which may in turn change the thermal resistance of the module, particularly during the later period of its operational lifetime. The resisting normal thermal-electronic thermal model is based on the fixed thermal parameters supported by power module manufacturers [6] and may not be suitable for the

⁴ Address for correspondence: H Li, Y G Hu, the State Key Laboratory of Power Transmission Equipment & System Security and New Technology (Chongqing University), Chongqing, China. E-mail: cqulh@163.com, huyaogang345@163.com



monitoring of the condition of the module in different lifetime periods. Thus, investigations of the thermal model of the base plate solder fatigue and thermal analysis have an important academic significance to the reliability evaluation and monitoring of the condition of wind power converters.

Some researchers have focused on the junction temperature and solder fatigue. The lumped parameter method is used to establish the thermal network model for transient thermal conduction [6]. In [7], the influences of the impulse load on the junction temperature of the IGBT module is compared under the current hysteretic control, SPWM, and SVPWM control methods. The multichip thermal effects on the power cycling ability of an IGBT module are considered, and the evaluation error among different thermal models is analysed in [8]. A method of monitoring the condition of wind turbines based on case temperature is proposed in [9–10]. However, these investigations cannot effectively calculate the junction temperature at different lifetimes because of the fixed thermal resistance assumption, and the relationship between the thermal parameters and solder fatigue remains unknown. Although [11] monitors the condition of a power module with variations in the junction temperature at different power cycling times, this power module still uses the fixed thermal resistance. In [12], the junction temperature is calculated by analysing the heat conduction path. However, extracting the aging thermal parameters from 2D analysis is insufficient and needs further improvement.

This study presents an improved thermal network model of IGBT modules that considers the effects of base plate solder fatigue in large wind turbine power converters. In Section II, the actual structure of an IGBT module and the coupling thermal structure 3D finite element model (FEM) are introduced. In Section III, the thermal resistance of the module is fully investigated, and its improved thermal network model is proposed. In Section IV, the FEM and improved thermal network model of the module are verified by comparing them with the actual case monitoring temperature and multiple FEM results, respectively. In Section V, the conclusion is presented.

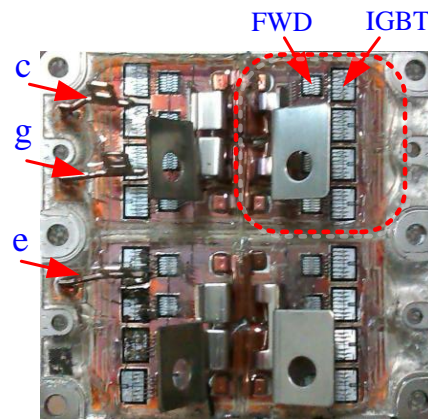
2. Actual structure of the IGBT module and FEM

2.1. Actual structure of the IGBT module

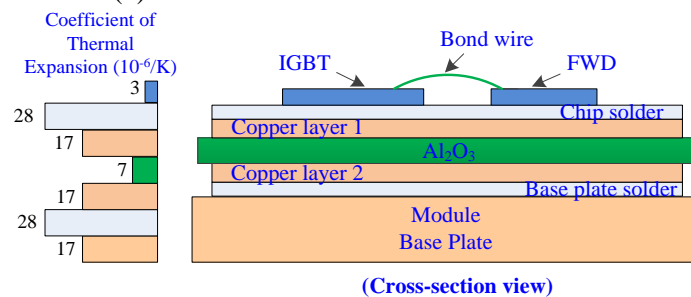
The actual structure of the IGBT module (FZ1600R17HP4) of a large-power doubly fed induction generator (DFIG) wind power converter is introduced to investigate comprehensively the IGBT module of a wind power converter. The inner structure of the wind power converter and the electrical connection of its IGBT module are shown in Figure 1. Figure 1 shows that each IGBT module consists of multiple IGBT chips and freewheeling diode (FWD) chips and that the structure of the layer of the IGBT module includes seven layers. Both the copper and ceramic layers comprise the direct bonded copper layer, which is connected to the base plate by the solder. Each layer of the IGBT module has different coefficients of thermal expansion (CTE), which result in the occurrence of alternating thermal stress between the two layers with temperature changes [13–15]. This kind of CTE mismatch causes fatigue cracks, which affect the heat dissipation of the IGBT chips. The concentration of extra temperature and the severe mechanical deformations enlarge the area of fatigue cracks and cause the desquamating part of the base plate solder.



(a) 2 MW DFIG wind power converter



(b) Inner structure of the IGBT module



(c) Cross-section view of the IGBT module

Figure 2. Chip sizes and FEM of the IGBT module

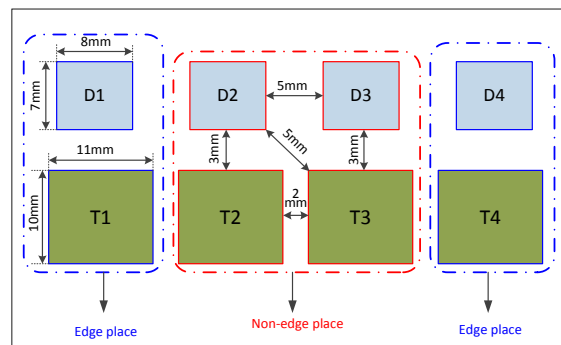
2.2. FEM of the IGBT module

The 3D FEM of the IGBT module is established with ANSYS to analyze further the relationship between thermal resistance and solder desquamation. According to the material properties of the IGBT module in Table 1 [16], the geometric model of the IGBT module is established with the tool of the design model in the ANSYS/workbench.

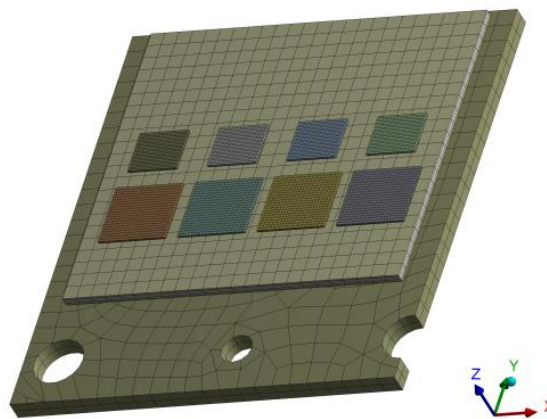
Table 1. Material properties of the IGBT module

IGBT module	Material	Thermal Conductivity $/W \cdot (m \cdot K)^{-1}$	Poisson's ratio	Young's modulus $/MPa$
IGBT	Si	139	0.28	112000
FWD	Si	139	0.28	112000
Solder1	Sn-Ag-Cu	78	0.4	43000
DCB Copper1	Cu	386	0.34	110000
Ceramic	Al_2O_3	18	0.22	370000
DCB Copper2	Cu	386	0.34	110000
Solder2	Sn-Ag-Cu	78	0.4	43000
Base Plate	Cu	386	0.34	110000

Given the structural symmetry and independence of its location, the 1/4 units marked with T1–T4 and D1–D4 of the whole IGBT module structure are chosen and investigated here. The sizes and distances of these chips are shown in Figure 2. (a), and the 3D FEM of the IGBT module is established, as shown in Figure 2. (b).



(a) Chip sizes of the IGBT module



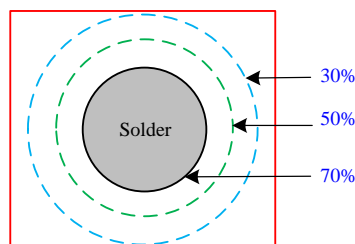
(b) FEM of the IGBT module

Figure 2. Chip sizes and FEM of the IGBT module

3. Thermal resistance increment and the improved thermal network model of the IGBT module

3.1. Thermal analysis of the IGBT module at different desquamating degrees

The junction temperature is analyzed to investigate the thermal resistance increment of the IGBT module in different solder fatigue periods by introducing the solder desquamating degree, which indicates the proportion of the desquamation area to the whole solder area, as shown in Figure 3.

**Figure 3.** Solder desquamating degree

If the wind speed is 12 m/s, then the power losses of the IGBT modules can be calculated with the power loss calculation equations described in [17], which are 2.27 W/mm³ in IGBT and 1.5 W/mm³ in FWD for this DFIG wind power converter. Each layer is presumably connected perfectly with no relative movements. The heat spreading through the silica gel is ignored. All heat flows also presumably derive from the active junctions and flow to the cooling air of the heat plate because of the sealed package. The ambient temperature is 50 °C. The above simulation condition is used for FEM, and the expected emulation result is obtained at different desquamating degrees of 0%, 30%, 50%, and 70%, as shown in Figure 4.

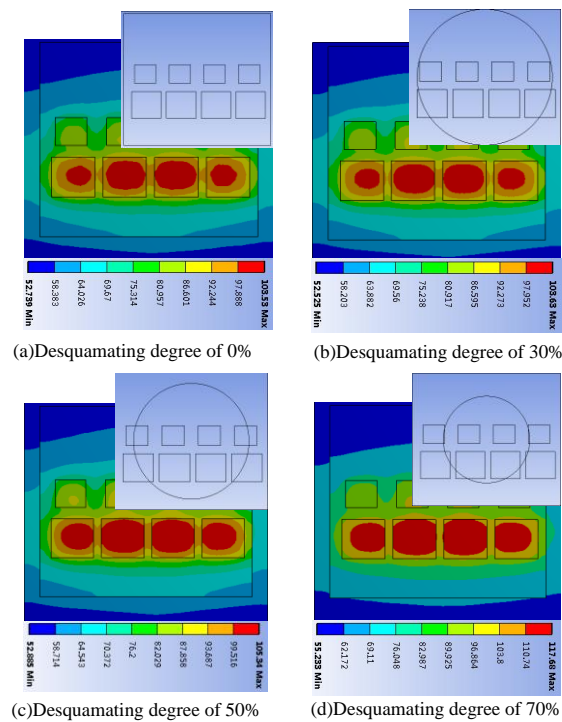


Figure 4. Temperature distribution of the IGBT module at different desquamating degrees of the base plate solder

Figure 4 shows that the junction temperature of IGBT changes slightly under the condition of 30% solder desquamating compared to that under the healthy condition of 0%. When the solder desquamation reaches 50%, the junction temperature of the IGBT is 105.3 °C, and the 2 °C increment is larger than that under the healthy condition. Although the junction temperature reaches 117.6 °C at the desquamating degree of 70%, the 14 °C increment is larger than that under the healthy condition. The junction temperature characteristics of IGBT caused by different solder desquamating conditions and wind speeds are also investigated, as shown in Figure 5. At the same solder desquamating degree, the junction temperature increases as the wind speed increases, as shown in Figure 5. At the same wind speed, the junction temperature of the IGBT also tends to increase as the solder desquamation increases, particularly when the solder desquamating degree reaches 50%.

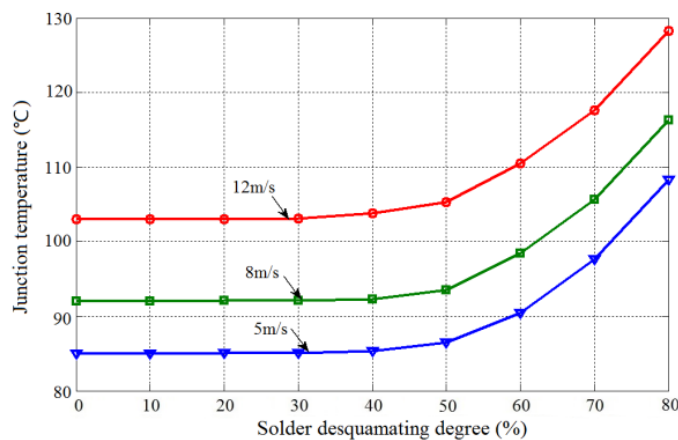


Figure 5. Junction temperature curves of the IGBT at different desquamating degrees of the base plate solder and wind speeds

3.2. Thermal resistance increment

To further investigate the relation of steady thermal resistance and solder fatigue, the junction to the case thermal resistance R_{th} can be described as follows:

$$R_{th} = \frac{T_j - T_c}{P} \quad (1)$$

The failure mechanism of the IGBT module results in a change in the fatigue thermal resistance $R_{th}(t)$ in different lifetime periods. The thermal resistance increment can be depicted as

$$\Delta R_{th}(t) = R_{th}(t) - R_{th0}, t \geq 0 \quad (2)$$

where R_{th0} means the steady thermal resistance of the IGBT module under healthy condition.

According to the simulation results of FEM at different solder desquamating degrees, a thermal resistance increment in the wind speed of 12 m/s is calculated with (1) and (2) to further determine the influence of the solder fatigue on the thermal resistance of the IGBT module; the results are shown in Table 2.

Table 2. Junction temperature and thermal resistance increment

Desquamating degree	$T_{j,IGBT}$ (°C)	ΔR_{th} (°C/W)	Proportion
0%	103.00	0	0%
10%	103.00	0	0%
20%	103.06	0.0002	0.10%
30%	103.09	0.0005	0.20%
40%	103.80	0.0038	1.57%
50%	105.30	0.0108	4.50%
60%	111.47	0.0348	14.50%
70%	117.63	0.0679	28.30%

The junction temperature and the thermal resistance increase as the solder desquamating degree increases. In general, the IGBT module is considered a failure when the thermal resistance increment reaches 20% [5, 9, 10]. The thermal resistance increment of the base plate solder slightly changes when the solder desquamating degree is within 30%. The reason is that the thermal conduction area is not influenced under that condition. However, the thermal resistance increment is 14.5% when the solder desquamating degree reaches 60%. It also tends to increase immediately. The thermal resistance increment curves at desquamating degrees of 5, 8, and 12 m/s are shown in Figure 6 to further study the influence of wind speed on thermal resistance.

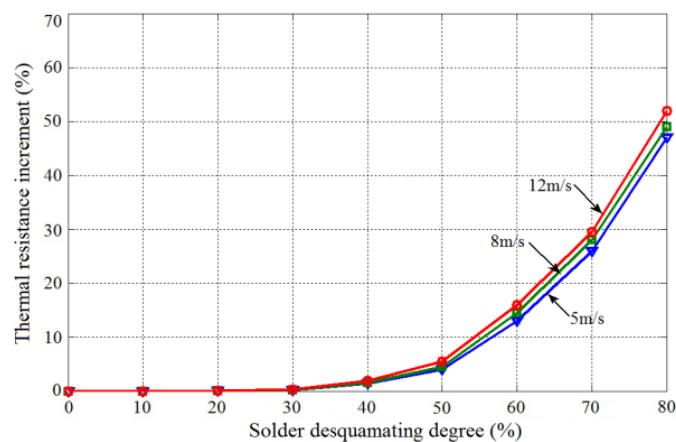


Figure 6. Thermal resistance increment of the IGBT at different solder desquamating degrees and wind speeds considering the change in thermal resistance.

Figure 6 illustrates that, at the same solder desquamating degree, wind speed apparently has no influence on thermal resistance increments, which are determined by different solder desquamating degrees.

3.3. Improved thermal network model

According to the structure of the layer of the IGBT module shown in Figure 1(c), the thermal impedance from the junction to case $Z_{th_{jc}}$ is modeled as a four-layer Foster RC network, as shown in Figure 7.

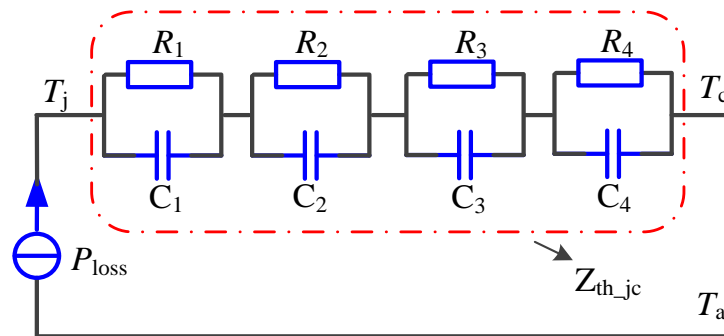


Figure 7. General foster thermal model of the IGBT module.

In Figure 7, the thermal resistance R_j determines the steady state mean value of the junction temperature, and the thermal capacitance C_j determines the dynamic change or fluctuation of the junction temperature. T_j and T_a denote the junction temperature and ambient temperature, respectively.

The thermal resistance increment must be considered during the process of thermal network modeling to accurately obtain the junction temperature of the IGBT module. According to the structure of the multiple IGBT chips and FWD chips at the base plate, the thermal resistance should be composed of inherent resistance increment R_{th-sc} and increment ΔR_{th-tr} when the heat transfer process of the IGBT module stabilizes and the thermal capacitance can be ignored. Thus, the improved thermal network model of the IGBT module is as shown in Figure 8.

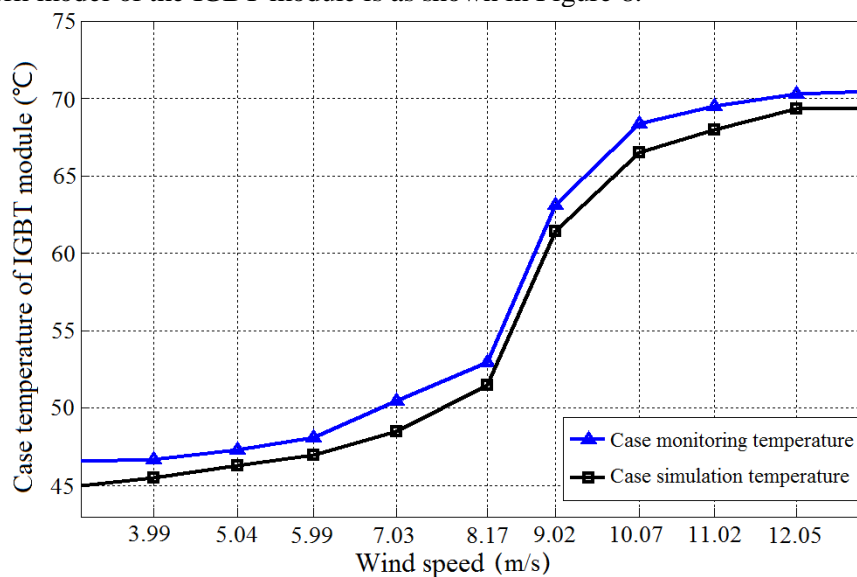


Figure 8. Improved thermal network model of the IGBT module considering the change in thermal resistance.

According to the improved thermal network model in Figure 8, R_{aged} is used as the junction case thermal resistance, which can be described as

$$R_{aged} = R_{th_{jc}} + \Delta R_{th} \quad (3)$$

Thus, the junction temperature of the IGBT module can be calculated with (4):

$$T_{j_{aged}} = P_{loss} \cdot (R_{th_{jc}} + \Delta R_{th}) + T_c \quad (4)$$

where $T_{j_{aged}}$ means the aged junction temperature, and P_{loss} denotes the power loss of the IGBT module.

4. Model validation

4.1. Validation of FEM

To further prove the effectiveness of the FEM and thermal analysis, the case temperature is calculated through FEM and compared with the actual case monitoring temperature of a 2 MW DFIG wind power converter without solder desquamation. The comparative results are depicted in Figure 9.

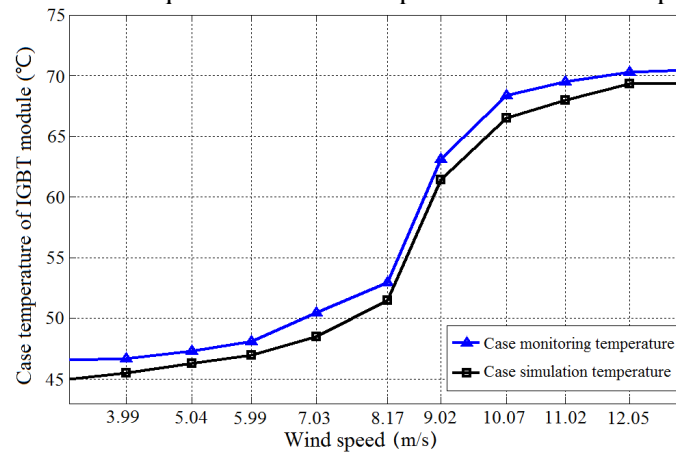


Figure 9. Monitoring data and simulation results of the IGBT module case temperature of a wind power converter.

The curve of the case monitoring temperature is obtained with the average case monitoring temperature at the same wind speed for 60 s, and the curve of the case simulation temperature is obtained through FEM. Figure 9 shows that the case temperature obtained through FEM matches the actual case monitoring temperature well under different operation conditions. This finding verifies the effectiveness of FEM and thermal analysis of the IGBT module.

4.2. Validation of the improved thermal network model

To verify the effectiveness of the thermal resistance increment and the proposed improved thermal network model, the improved thermal network model of the IGBT module is established in PLECS. The junction temperature of the IGBT module at different solder desquamation degrees is also calculated at the wind speeds of 6.8, 11.3, and 12 m/s. The simulation results with the same power losses are also calculated for comparison, as shown in Figure 10. The steady junction temperature of the IGBT with the improved thermal network model that considers the effects of solder fatigue matches the FEM thermal results well under the same operational condition. This finding further verifies the effectiveness of the improved thermal network model. Because the result from the thermal network is the mean value, whereas that from FEM is the maximum value, the two curves are slightly different.

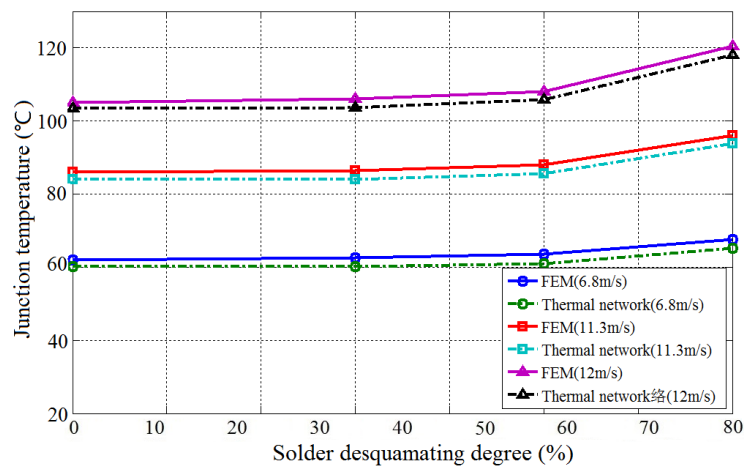


Figure 10. Comparison of the junction temperature of the IGBT at different fatigue stages.

5. Conclusion

This study proposes an improved thermal network model of the IGBT model for wind power converters, which considers the effects of base plate solder fatigue. The junction temperature and thermal resistance are analysed at different solder desquamating degrees through the proposed FEM. The actual case temperature and simulation results are used to verify the effectiveness of the improved thermal network model. The simulation results show that the junction temperature increases as the solder desquamating degree increases under the same operational condition. The thermal resistance increment also increases as the solder desquamation increases, and the junction temperature of the IGBT module can be calculated effectively with the proposed improved thermal network model. The proposed model is further verified with the FEM thermal results under multiple operational conditions. The future work will be to study the calculation of junction temperature considering effects of chip solder fatigue.

Acknowledgments

This study was supported by the Chongqing Graduate Student Research Innovation Project (CYB14014), the International Science and Technology Cooperation Program of China (2013DFG61520), the Fundamental Research Funds for the Central Universities (CDJXS10151152), the Fundamental Research Funds for the Central Universities (CDJZR12150074), and the Integration and Demonstration Program of Chongqing (CSTC2013JCSF70003). The authors are grateful for the supports.

References

- [1] Oshaba A S and Ali E S 2013 *Research Journal of Applied Sciences Engineering & Technology* **18** 4594-606
- [2] E. S. Ali 2015 *Energy* **89** 593-600
- [3] Yang S Y, Angus Bryant, Philip Mawby, Xiang D W, Ran L and Tavner P 2011 *IEEE Transactions on Industry Applications* **47** 1441-51
- [4] Blaabjerg F, Liserre M, and Ma K 2012 *IEEE Transactions on Industry Applications* **48** 708-19
- [5] Yang S, Xiang D, Bryant A, Mawby P A, Ran L and Tavner P J. 2010 *IEEE Transactions on Power Electronics* **25** 2734-52
- [6] Wei K X and Du M X 2011 *Transactions of China Electrotechnical Society* **26** 79-84
- [7] Nejadpak A, Mirafzal B, Mohammed O and Lixiang W 2010 *IECON Annual Conference on IEEE Industrial Electronics Society* (Glendale, Arizona, USA) **36** 451-6
- [8] Poller T, D'Arco S, Hernes M and Lutz J 2012 *International Conference on Integrated Power Electronics Systems* (Nuremberg, German) 1-6

- [9] Xiang D, Ran L, Tavner P J, Bryant A, Yang S and Mawby P 2011 *IEEE Transactions on Industry Applications* **47** 2578-91
- [10] Tian B, Wang Z and Qiao W 2014 *IEEE Applied Power Electronics Conference and Exposition–Apec* (TX, USA) 2564-68
- [11] Tian B, Qiao W, Wang Z, Gachovska T and Hudgins J L 2014 *IEEE Applied Power Electronics Conference and Exposition–Apec* (TX, USA) 2550-55
- [12] Wang Z, Qiao W, Tian B and Qu L Y 2014 *IEEE Applied Power Electronics Conference and Exposition–Apec* (TX, USA) 513-8
- [13] Ciappa M. 2002 *Microelectronics Reliability* **42** 653-667
- [14] Guo H, Watson S, Tavner P and Xiang J 2009 *Reliability Engineering & System Safety* **94** 1057-63
- [15] Tang Y, Wang B, Chen M and Liu B 2014 *Transactions of China Electrotechnical Society* **29** 17-23
- [16] Wintrich A, Nicolai U, Tursky W, and Reimann T 2011 *Application manual power semiconductors* (Nuremberg: ISLE Verlag)
- [17] Mao P, Xie S J and Xu Z G 2010 *Pro of the CSEE* **30** 40-47